Deletion of periostin reduces muscular dystrophy and fibrosis in mice by modulating the transforming growth factor-β pathway

Angela Lorts[a,1], Jennifer A. Schwanekamp[a,1], Troy A. Baudino[b], Elizabeth M. McNally[c], and Jeffery D. Molkentin[a,d,2]

[a]Department of Pediatrics, Cincinnati Children's Hospital, University of Cincinnati, Cincinnati, OH 45229; [b]Department of Medicine, Texas A&M Health Science Center College of Medicine, Temple, TX 76504; [c]Department of Medicine, University of Chicago, Chicago, IL 60637; and [d]Howard Hughes Medical Institute, Cincinnati Children's Hospital, Cincinnati, OH 45229

Edited by Kevin P. Campbell, University of Iowa Carver College of Medicine, Iowa City, IA, and approved May 18, 2012 (received for review March 20, 2012)

The muscular dystrophies are broadly classified as muscle wasting diseases with myofiber dropout due to cellular necrosis, inflammation, alterations in extracellular matrix composition, and fatty cell replacement. These events transpire and progress despite ongoing myofiber regeneration from endogenous satellite cells. The degeneration/regeneration response to muscle injury/disease is modulated by the proinflammatory cytokine transforming growth factor-β (TGF-β), which can also profoundly influence extracellular matrix composition through increased secretion of profibrotic proteins, such as the matricellular protein periostin. Here we show that up-regulation and secretion of periostin is pathological and enhances disease in the δ-sarcoglycan null (*Sgcd*$^{-/-}$) mouse model of muscular dystrophy (MD). Indeed, MD mice lacking the *Postn* gene showed dramatic improvement in skeletal muscle structure and function. Mechanistically, *Postn* gene deletion altered TGF-β signaling so that it now enhanced tissue regeneration with reduced levels of fibrosis. Systemic antagonism of TGF-β with a neutralizing monoclonal antibody mitigated the beneficial effects of *Postn* deletion in vivo. These data suggest that periostin functions as a disease determinant in MD by promoting/allowing the pathological effects of TGF-β, suggesting that inhibition of periostin could represent a unique treatment approach.

collagen | transgenic mice | dystrophin-glycoprotein complex | paracrine

Muscular dystrophy (MD) broadly encompasses a diverse group of genetic disorders that result in loss of muscle fibers, leading to progressive skeletal muscle weakness, dilated cardiomyopathy, and premature death (1). The majority of genetic mutations identified in patients with MD appear to affect the multiprotein sarcolemmal-spanning dystrophin-glycoprotein complex, which is critical for stabilization of the membrane and prevention of calcium overload, leading to myofiber death and an inflammatory response (2). One such inflammatory mediator, transforming growth factor (TGF)-β, is thought to worsen MD and lead to increased fibrosis in human dystrophic muscle (3, 4) and animal models of dystrophy (5); for example, administration of decorin (a TGF-β antagonist) reduces collagen expression in the diaphragm of dystrophin-deficient *mdx* mice (6), and losartan (an angiotensin II type 1 receptor blocker thought to reduce TGF-β activity) normalizes muscle architecture and improves function in animal models of myopathy (7, 8). Recently, genetic alterations in the TGF-β pathway, such as changes in latent TGF-β binding protein 4, also have supported the theory of a strong interplay between TGF-β–induced fibrosis and MD severity (9). In vitro, TGF-β can directly influence satellite cell proliferation, myocyte differentiation, and myofiber fusion (10).

Periostin is a 90-kDa secreted extracellular matrix (ECM) protein that has been proposed to function upstream and downstream of TGF-β (11). It contains four fasciclin domains that are also observed in the insect protein fasciclin I, which is involved in neuronal cell–cell adhesion (11, 12). Periostin expression is low at baseline in many adult tissues, but is strongly induced and secreted into the ECM after acute injury, as well as in dystrophic skeletal muscle (13). Periostin is expressed exclusively by fibroblasts or cells that adopt a fibroblast-like phenotype after an injurious event (14). In the heart, we and others have shown that periostin is strongly induced after myocardial infarction and left ventricular pressure overload, where it plays a role in ECM remodeling and healing (15, 16).

In the present study, we found that mice lacking periostin (*Postn*) were profoundly protected from MD through mechanisms involving decreased fibrosis and enhanced myofiber regeneration in conjunction with increased TGF-β activity. Although inhibition of TGF-β is typically protective in MD, the protection that we observed in dystrophic mice lacking *Postn* was reversed by administration of a TGF-β–blocking antibody, suggesting another example of the so-called "TGF-β paradox" (17). Thus, therapeutic manipulation of periostin may offer another means of altering MD disease progression when TGF-β responsiveness is targeted.

Results

Periostin Is Induced in Dystrophic Skeletal Muscle. Periostin is normally expressed in low amounts in adult tissues, but expression is dramatically increased after, for example, myocardial infarction simultaneously with the fibrotic response and scar formation (16). MD is characterized by ECM remodeling, fibrosis, and progressive scarring in skeletal muscle, suggesting that periostin could be similarly involved. Indeed, biopsy material from human skeletal muscle of a patient with Duchenne MD showed periostin accumulation by immunohistochemistry in the ECM within an area of myofiber dropout (Fig. 1*A*). Similarly, we also analyzed *Sgcd*$^{-/-}$ mice, a model of MD that arises due to deletion of the δ-sarcoglycan protein (18). Serum from these mice demonstrated increased circulating levels of periostin by ELISA (Fig. 1*B*), as well as by Western blot analysis of diseased skeletal muscle (Fig. 1*C*). Immunohistochemistry analysis revealed profound induction and accumulation of periostin in the ECM of the diaphragm, gastrocnemius, and quadriceps at 6 wk and 6 mo of age (Fig. 1*D*). In the heart, cardiac fibroblasts were found to be the source of periostin; thus, to discern the cell type expressing periostin in our dystrophic model, we used a transgene containing the periostin promoter driving ZsGreen. We observed that only the interstitial cells expressed periostin in

Author contributions: A.L. and J.D.M. designed research; A.L. and J.A.S. performed research; T.A.B. and E.M.M. contributed new reagents/analytic tools; and A.L., J.A.S., and J.D.M. wrote the paper.

The authors declare no conflict of interest.

This article is a PNAS Direct Submission.

[1]A.L. and J.A.S. contributed equally to this work.

[2]To whom correspondence should be addressed. E-mail: jeff.molkentin@cchmc.org.

This article contains supporting information online at www.pnas.org/lookup/suppl/doi:10.1073/pnas.1204708109/-/DCSupplemental.

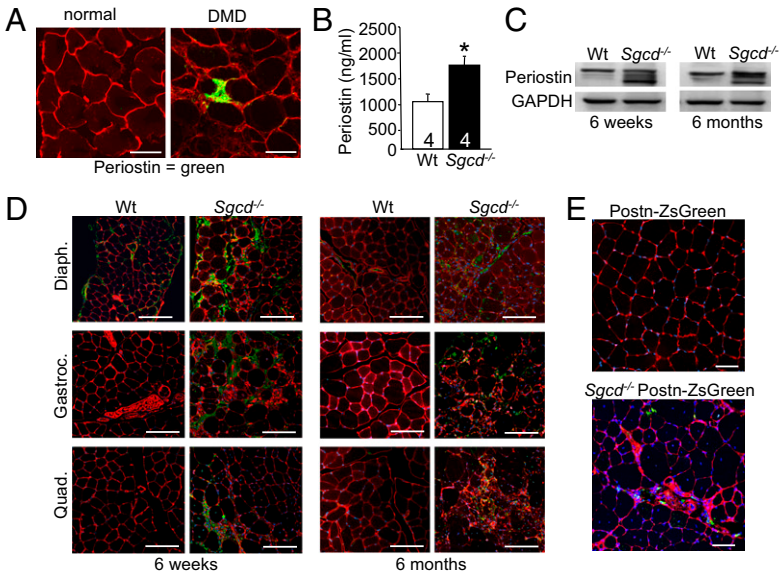

Fig. 1. Evaluation of periostin expression in $Sgcd^{-/-}$ mice. (*A*) Immunohistochemistry showing periostin (green) localization in muscle biopsy specimens from normal patients and patients with Duchenne MD (DMD). (Original magnification: 600×; scale bar: 50 μm.) (*B*) Periostin levels, detected by ELISA, in the serum of 6-wk old WT (Wt) and $Sgcd^{-/-}$ mice. *$P < 0.05$. $n = 4$ mice each. (*C*) Western blot for periostin in Wt and $Sgcd^{-/-}$ mice from the diaphragm at 6 wk and 6 mo of age. GAPDH was used as a loading control. (*D*) Immunohistochemistry showing increased periostin (green) in areas of fibrosis in the diaphragm (diaph.), gastrocnemius (gastroc.), and quadriceps (quad.) of Wt and $Sgcd^{-/-}$ mice at 6 wk and 6 mo of age. Membranes are stained in red with wheat germ agglutinin conjugated to TRITC, and nuclei are stained with DAPI (blue). (Original magnification: 400×; scale bar: 100 μm.) (*E*) Immunohistochemistry showing ZsGreen staining (green) of the gastrocnemius in $Sgcd^{-/-}$ and $Sgcd^{-/-}$Postn-ZsGreen TG mice. The ZsGreen-positive cells express periostin. Wheat germ agglutinin was conjugated to TRITC (red) and To-Pro nuclei (blue). Error bars represent SEM.

dystrophic skeletal muscle (Fig. 1*E*). Immunohistochemistry showed that the ZsGreen signal overlapped with ∼70–80% of the resident fibroblasts as marked with a pan-fibroblast polyclonal antisera, anti-vimentin, and α-smooth muscle actin for activated fibroblasts (Fig. S1). These data indicate that periostin is induced in fibroblasts in diseased skeletal muscle.

Deletion of Periostin Ameliorates MD Histopathology in $Sgcd^{-/-}$ Mice. We hypothesized that the ablation of *Postn* would reduce the pathogenesis of MD by limiting fibrosis, thereby enhancing ongoing regeneration or perhaps limiting the inflammatory response. Indeed, deletion of *Postn* in the $Sgcd^{-/-}$ mouse background showed substantially less histopathology at both 6 wk and 6 mo of age in the diaphragm, gastrocnemius, and quadriceps compared with $Sgcd^{-/-}$ mice, whereas Wt and $Postn^{-/-}$ mice demonstrated no disease (Fig. S2). An increase in muscle weight due to pseudohypertrophy is associated with MD; this was observed in muscles from $Sgcd^{-/-}$ mice at 6 wk and 6 mo of age, but not in $Sgcd^{-/-}Postn^{-/-}$ mice (Fig. 2 *A* and *B*). Interestingly, quantification of central nucleation from histological muscle sections, which typically reflects ongoing myofiber regeneration or the total amount of damage, showed equal or elevated levels in $Sgcd^{-/-}Postn^{-/-}$ mice compared to $Sgcd^{-/-}$ mice, suggesting that loss of *Postn* did not limit myofiber regeneration or damage

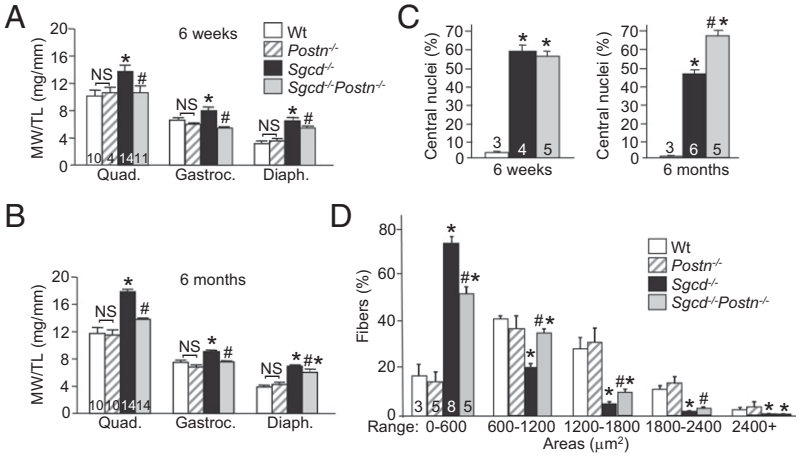

Fig. 2. Genetic deletion of periostin diminishes the pathology in $Sgcd^{-/-}$ muscle. (*A* and *B*) Muscle weights normalized to tibia length from the quadriceps, gastrocnemius, and diaphragm in the indicated groups of mice at 6 wk and 6 mo of age. (*C*) Quantification of the percent of fibers containing central nuclei in the gastrocnemius from 6-wk-old and 6-mo-old mice. (*D*) Fiber areas from the gastrocnemius of the indicated mice separated into ranges. Error bars represent SEM. *$P < 0.05$ vs. Wt; #$P < 0.05$ vs. $Sgcd^{-/-}$. The numbers of mice or muscles analyzed are shown in the bars.

(Fig. 2*C*). Myofibers from *Sgcd*$^{-/-}$*Postn*$^{-/-}$ mice were significantly larger across different ranges of cross-sectional areas compared with those from *Sgcd* $^{-/-}$ mice, suggesting more orderly regeneration, likely due to less tissue fibrosis and pathological ECM remodeling (Fig. 2*D*). Indeed, direct assessment of tissue fibrosis with Masson's trichrome histological staining of diaphragm, gastrocnemius, and quadriceps at 6 wk and 6 mo of age showed significant reductions in *Sgcd*$^{-/-}$*Postn*$^{-/-}$ mice compared with single-null *Sgcd* mice (Fig. 3 *A*–*C*). Measurement of total tissue hydroxyproline content in the quadriceps confirmed these histological findings (Fig. 3*D*). Along with less fibrosis, skeletal muscle from *Sgcd*$^{-/-}$*Postn*$^{-/-}$ mice showed a dramatic up-regulation in the expression and activity of matrix metalloproteinase 9 (MMP9), which enhances ECM turnover to maintain tissue plasticity and beneficial remodeling (Fig. 3 *E* and *F*). Other positive effects observed in skeletal muscle from double-null mice compared with single-null *Sgcd* mice included reduced mRNA levels of collagen 5α3 and 1α2 (Fig. 3*G*). Collectively, these results suggest that loss of *Postn* improves skeletal muscle tissue pathology through beneficial ECM remodeling and reduced fibrosis, as well as enhanced regeneration.

Deletion of *Postn* Ameliorates Broader Indexes of MD in *Sgcd*$^{-/-}$ Mice. In addition to less pathology at the histological level in skeletal muscle, *Sgcd*$^{-/-}$*Postn*$^{-/-}$ mice showed a profound reduction in total serum creatine kinase levels at age 6 wk and 6 mo compared with *Sgcd*$^{-/-}$ mice, suggesting less myofiber membrane ruptures, possibly due to more uniform ECM properties with less inflammation (Fig. 4 *A* and *B*). This profile of healthier skeletal muscle in *Sgcd*$^{-/-}$*Postn*$^{-/-}$ mice compared to *Sgcd*$^{-/-}$ mice also correlated with better functional performance; the double-null mice exercised significantly longer with forced treadmill running compared with the single-null *Sgcd* mice (Fig. 4 *C* and *D*). Collectively, these results indicate that deletion of *Postn* enhances myofiber integrity in *Sgcd* deleted mice, resulting in better functional performance.

Although serum creatine kinase levels were reduced in *Sgcd*$^{-/-}$*Postn*$^{-/-}$ mice compared with single-null *Sgcd* mice, suggesting fewer membrane ruptures, overall levels of myofiber turnover were likely the same in the two types of mice, given that central nucleation was either the same or even enhanced in the double-null mice (Fig. 2*C*). Indeed, quantitation of myofibers expressing embryonic myosin heavy chain (eMHC) or myogenin, which demarcates newly regenerated fibers, showed higher levels in *Sgcd*$^{-/-}$*Postn*$^{-/-}$ mice compared with single-null *Sgcd* mice, suggesting enhanced regeneration (Fig. 5*A*). The simplest interpretation of all of the data presented to this point is that myofiber degeneration is no different between *Sgcd*$^{-/-}$*Postn*$^{-/-}$ mice and single-null *Sgcd* mice. However, by reducing the accumulation of fibrotic material, ECM "health" is maintained, which permits greater levels of ongoing regeneration with fewer secondary ruptures in myofiber membranes. Such observations also should be consistent with less ongoing inflammation, which we examined directly in this study. Indeed, *Sgcd*$^{-/-}$*Postn*$^{-/-}$ mice had significantly fewer macrophages in histological sections from skeletal muscles compared with single-null *Sgcd* mice (Fig. 5 *B*–*D*).

Altered TGF-β Signaling Underlies Periostin-Dependent Effects on MD. Periostin expression is known to be induced by TGF-β and to affect TGF-β signaling. Thus, we analyzed TGF-β levels and the activation of downstream transcription factors, such as Smad2/3, that are regulated by TGF-β. Inhibition of TGF-β has been shown to reduce aspects of MD disease in skeletal muscle, because it is typically induced during MD, as we confirmed here in *Sgcd*$^{-/-}$ muscle (6–8) (Fig. 5*E*). More importantly, deletion of *Postn* in the *Sgcd*$^{-/-}$ background led to significantly higher TGF-β levels in skeletal muscle (Fig. 5*E*). Consistent with these results, use of a phospho-specific Smad2/3 antibody on muscle histological sections produced greater levels of activation in

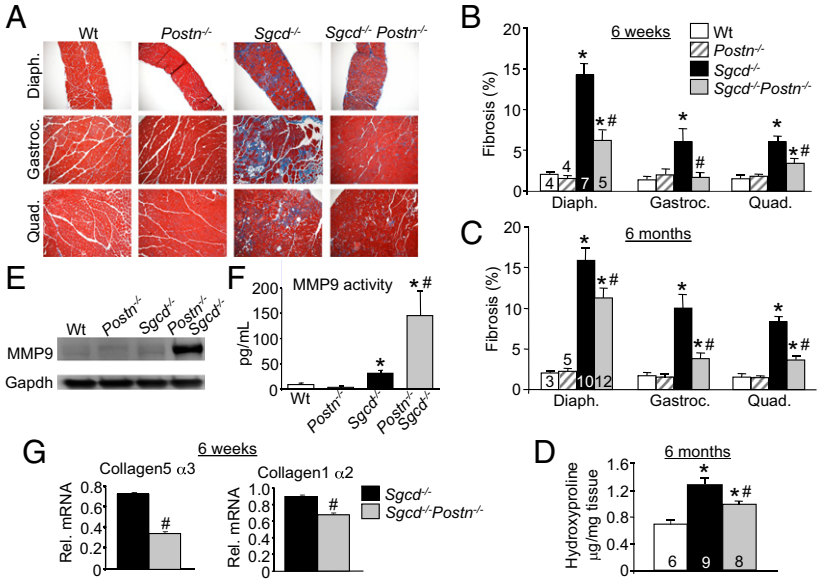

Fig. 3. Analysis of the ECM in skeletal muscle. (*A*) Representative Masson's trichrome-stained diaphragm, gastrocnemius, and quadriceps from WT, *Postn*$^{-/-}$, *Sgcd*$^{-/-}$, and *Sgcd*$^{-/-}$*Postn*$^{-/-}$ mice at 6 mo of age. (Original magnification: 100×.) (*B* and *C*) Quantification of fibrotic area by Masson's trichrome staining at 6 wk and 6 mo of age. The number of muscles analyzed is shown in the bars. (*D*) Measurement of hydroxyproline content in the quadriceps from WT, *Sgcd*$^{-/-}$, and *Sgcd*$^{-/-}$*Postn*$^{-/-}$ mice expressed as micrograms of hydroxyproline per milligram of tissue. (*E*) Western blot analysis for MMP9 in the indicated groups of mice from the gastrocnemius at 6 wk of age. GAPDH was used as a loading control. (*F*) MMP9-specific activity assay from the gastrocnemius of the indicated mice (6 wk of age). $n = 3$ or more for each group. (*G*) Real-time PCR from quadriceps muscle of the indicated mRNA in *Sgcd*$^{-/-}$ vs. *Sgcd*$^{-/-}$*Postn*$^{-/-}$ mice. mRNA levels were normalized to 18s RNA. Error bars represent SEM. $^{*}P < 0.05$ vs. WT; $^{\#}P < 0.05$ vs. *Sgcd*$^{-/-}$. The number of mice analyzed is shown in or above the bars.

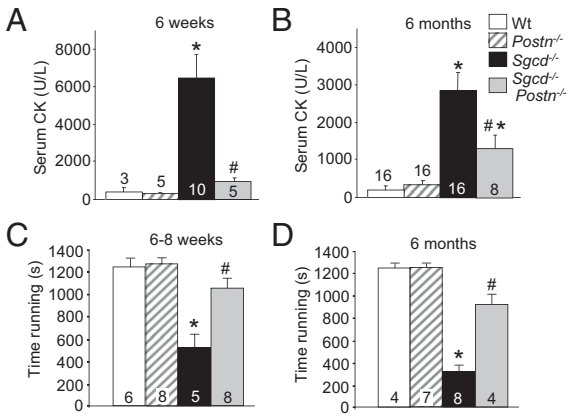

Fig. 4. Loss of periostin improves in vivo muscle function. (*A* and *B*) Quantification of serum creatine kinase (CK) levels in the indicated groups of mice at 6 wk and 6 mo of age. (*C* and *D*) Time to fatigue in seconds with forced downhill treadmill running in the indicated groups of mice. Error bars represent SEM. $^{*}P < 0.05$ vs. WT; $^{\#}P < 0.05$ vs. $Sgcd^{-/-}$. The number of mice analyzed is shown in or above the bars.

$Sgcd^{-/-}Postn^{-/-}$ mice compared with single-null *Sgcd* mice at 6 wk of age, suggesting enhanced TGF-β signaling (Fig. 5 *F* and *G*). To mechanistically assess whether this increase in TGF-β influencesd the protection observed in skeletal muscle of $Sgcd^{-/-}Postn^{-/-}$ mice, we used a TGF-β–blocking monoclonal antibody as a systemic treatment. Six weeks of this treatment lead to a decrease in Smad2/3 phosphorylation in skeletal muscle of $Sgcd^{-/-}Postn^{-/-}$ mice, indicating nearly complete inhibition of TGF-β signaling (Fig. 6*A*). As suggested previously in the literature, treatment of *mdx* mice with the TGF-β pathway inhibitor losartan partially mitigated MD phenotypic manifestations (7, 8). In contrast, inhibition of TGF-β signaling in $Sgcd^{-/-}Postn^{-/-}$ mice significantly worsened muscle function, such that these mice now had reduced exercise capacity compared with those receiving vehicle treatment (Fig. 6*B*). The deleterious effects of TGF-β blockade in the $Sgcd^{-/-}Postn^{-/-}$ mice may be related to the TGF-β paradox described in the oncology literature (17), which in skeletal muscle may reflect an interplay between myofiber regeneration versus ongoing fibrosis and ECM remodeling. Indeed, assessment of regeneration by reexpression of MyoD, myogenin, and Pax7 in the different groups of mice suggested that TGF-β–neutralizing antibody enhanced regeneration in single-null *Sgcd* mice, but inhibited regeneration in $Sgcd^{-/-}Postn^{-/-}$ mice (Fig. 6*C*).

The foregoing results suggest that in the absence of *Postn*, TGF-β signaling is altered so as to support regeneration without an increase in tissue fibrosis. To more directly examine this concept, we analyzed regeneration in $Postn^{-/-}$ mice versus WT mice over a 21-d period after freeze injury. Periostin protein induction was evident within 3 d after freeze injury, became more elevated by 7 d, and then was nearly absent by 21 d (Fig. 6*D*). Assessment of eMHC- and myogenin-positive fibers in the area of freeze injury suggested greater myofiber regeneration in $Postn^{-/-}$ muscle compared with WT muscle, as well as a greater percentage of the smaller regenerative myofibers (<100 μm^2) (Fig. 6 *E*–*G*). Gross histological assessment of the injury area also demonstrated faster and more complete healing in $Postn^{-/-}$ muscle after freeze injury compared with WT controls. These findings indicate that loss of *Postn* leads to improved myofiber regeneration in conjunction with a reprogramming of TGF-β function in diseased skeletal muscle.

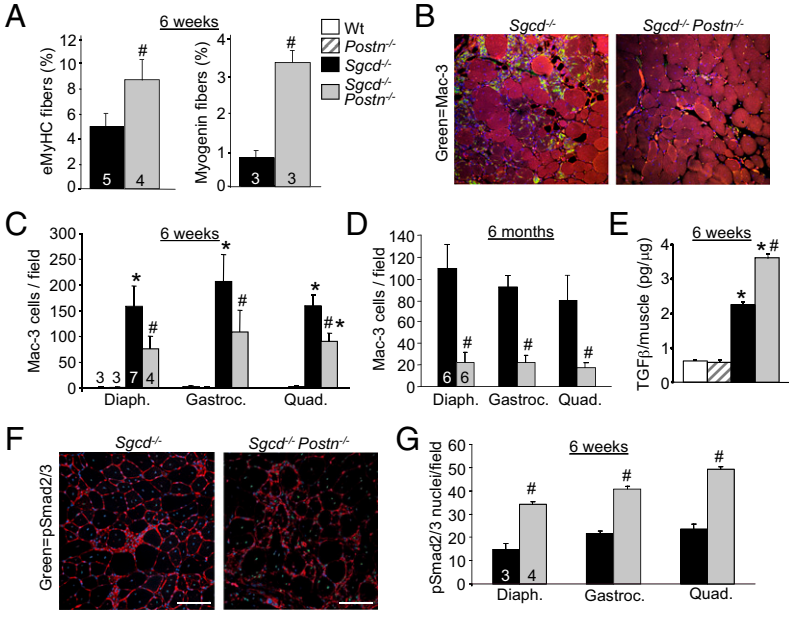

Fig. 5. Loss of periostin improves skeletal muscle regeneration in dystrophic mice. (*A*) Quantification of the percent of embryonic myosin heavy chain (eMHC)-positive fibers and myogenin-positive nuclei in the gastrocnemius of $Sgcd^{-/-}$ and $Sgcd^{-/-}Postn^{-/-}$ mice at 6 wk of age. (*B*) Representative immunohistochemical images for the activated macrophage marker Mac-3 (green cells) in the gastrocnemius muscle of $Sgcd^{-/-}$ and $Sgcd^{-/-}Postn^{-/-}$ mice at 6 mo of age. Red staining was with WGA-TRITC, and blue denotes nuclei (TO-PRO). (Original magnification: 400×.) (*C* and *D*) Quantification of Mac-3–positive cells per field in the indicated groups of mice at 6 wk and 6 mo of age. (*E*) ELISA detection of TGF-β levels in the quadriceps of 6-wk old WT and $Sgcd^{-/-}$ mice. (*F*) Immunohistochemistry of phosphorylated (p) Smad2/3 (green nuclei) in the quadriceps of $Sgcd^{-/-}$ and $Sgcd^{-/-}Postn^{-/-}$ mice at 6 wk of age. Membranes are stained red with WGA-TRITC, and nuclei are stained blue with DAPI. (Scale bar: 100 μm.) (*G*) Quantification of percentage of phospho-Smad2/3–positive nuclei in the diaphragm, gastrocnemius, and quadriceps of $Sgcd^{-/-}$ and $Sgcd^{-/-}Postn^{-/-}$ mice at 6 wk of age. $^{*}P < 0.05$ vs. WT; $^{\#}P < 0.05$ vs. $Sgcd^{-/-}$. Error bars represent SEM. The numbers of mice or individual muscles examined are shown in or above the bars throughout the figure.

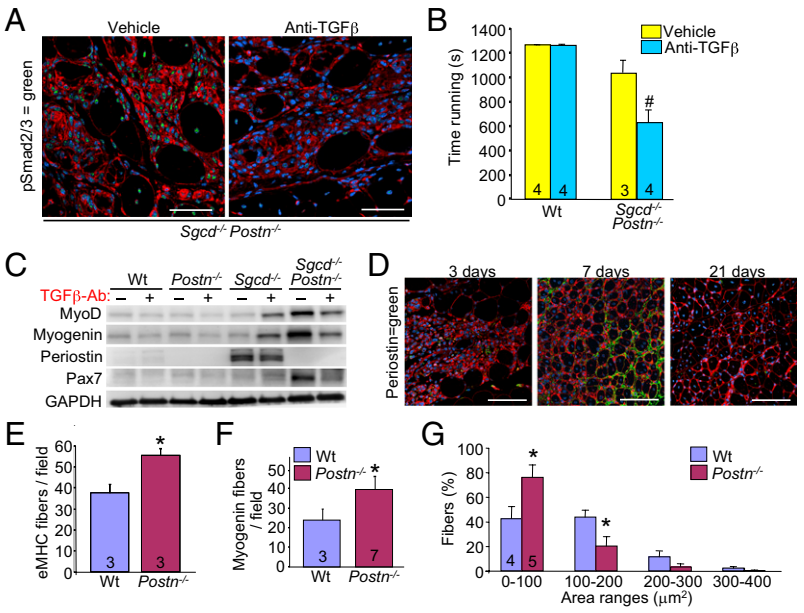

Fig. 6. Periostin leads to altered regeneration through TGF-β signaling in MD and muscle injury. (*A*) Representative immunohistochemistry of phospho-Smad2/3 in the quadriceps showing the nearly complete loss of signal in *Sgcd*$^{-/-}$*Postn*$^{-/-}$ mice injected with TGF-β neutralizing antibody. Original magnification: 600×; scale bar: 50 μm.) (*B*) Time to fatigue in seconds with forced downhill treadmill running in the indicated groups of mice injected with anti–TGF-β or vehicle. $^{\#}P < 0.05$, *Sgcd*$^{-/-}$*Postn*$^{-/-}$ vehicle vs. anti-TGF-β. (*C*) Western blots for MyoD, myogenin, periostin, and Pax7 in the gastrocnemius of the indicated groups of mice, injected or not injected with TGF-β antibody. GAPDH was used as a loading control. (*D*) Immunohistochemistry showing increased periostin (green) staining after 7 d of freeze injury in the gastrocnemius muscle. Red staining was with WGA-TRITC, and blue denotes nuclei (DAPI). (Original magnification: 400×; scale bar: 100 μm.) (*E*) Quantification of eMHC-positive fibers in the injured area of WT and *Postn*$^{-/-}$ mice after 7 d of injury. (*F*) Quantification of myogenin-positive nuclei in the injured area of WT and *Postn*$^{-/-}$ mice after 7 d of injury. (*G*) Fiber areas from the peri-injury area in the gastrocnemius of WT and *Postn*$^{-/-}$ mice, separated into ranges. $^{*}P < 0.05$ vs. WT; $^{\#}P < 0.05$ vs. vehicle. Error bars represent SEM. The numbers of mice or individual muscles examined are shown in or above the bars throughout the figure.

Discussion

The data presented here provide genetic evidence supporting the role of periostin in the pathogenesis of skeletal muscle injury, and marks this protein as a therapeutic target for the management of MD. Although this is unique in describing the benefit of *Postn* deletion in injured skeletal muscle, our results are consistent with, and provide mechanistic insight into, previous studies of cardiac muscle injury. In those studies, mice lacking *Postn* were much more likely to die after myocardial infarction injury due to a deficit in the fibrotic process and the inability to form a proper scar, which led to wall rupture; however, mice lacking *Postn* also demonstrated preserved cardiac function with long-term disease-inducing stimuli, likely because of less pathological remodeling of the ECM and accumulation of fibrotic material (15, 16). Previous work has strongly supported a direct interaction between periostin and ECM proteins such as fibronectin, tenascin-C, collagen I, collagen V, and heparin (19), suggesting that secretion of periostin might change the properties of these proteins or their assembly in the ECM. Indeed, the strength of collagen in the ECM is reduced in *Postn*-deficient mice (20, 21). Similar to the cardiac data, dystrophic mice deficient in *Postn* also exhibit beneficial changes in function, as well as dramatically decreased fibrosis. These observations suggest that the induction of periostin could be correlated with muscle pathology and disease severity in humans. To directly examine this, in previous work we queried the expression of periostin mRNA in a dataset of 125 human muscle biopsy specimens (22, 23). Of the 10 muscle diseases studied, nearly all were associated with increased periostin levels relative to normal muscle (Fig. S3). The most significant increases were in patients with Duchenne MD ($P < 0.0001$) and juvenile dermomyositis ($P < 0.0001$). Furthermore, the literature supports that the increase in periostin mRNA levels in Duchenne MD muscle is age-dependent and is elevated most significantly (a twofold increase) in young children (24).

Our results indicate that periostin negatively impacts disease pathogenesis in MD, such that its deletion enhances myofiber regeneration. These observations are superficially in direct opposition to a previous report in which direct application of a truncated version of periostin protein onto infarcted rodent hearts led to increased healing of the injury by induction of regeneration and cell cycle reentry of cardiomyocytes (25). However, a follow-up to that study found that overexpression of full-length periostin in vitro and in vivo did not alter the regeneration ability of the cardiomyocytes (26). Furthermore, periostin-overexpressing hearts (full-length protein) showed either baseline pathology or an increase in long-term fibrosis or hypertrophy, or worsening function with disease stimulation (16, 27). One interesting possibility that could explain the discordance between these studies is if the truncated version of periostin used by Kuhn et al. (25) actually had some sort of inhibitory activity toward periostin function, given that it lacks part of the N terminus and more than 140 amino acids of the C terminus. If this truncated version of periostin indeed disrupted key interactions observed with the full-length protein, such as its interaction with other ECM proteins, integrins, or even TGF-β, this would suggest a possible therapeutic advantage of applying this peptide to areas of injury as a periostin antagonist. Regardless of the reasons, our current results clearly demonstrate that loss of periostin is of benefit to diseased skeletal muscle in association with better myofiber regeneration, consistent with the results reported by Oka et al. (16) and Lorts et al. (26), in which hearts of periostin-overexpressing mice did not exhibit greater regeneration and were predisposed to disease.

We hypothesized that the changes in the ECM of *Postn*$^{-/-}$ mice allow for a more stable and favorable milieu for myocyte

regeneration. This hypothesis is supported by previously published data showing that *Postn*$^{-/-}$ mice have disorganized and dysfunctional collagen fibrils, leading to a less rigid ECM (21). In the oncologic literature, periostin has been shown to affect the ability of cells to migrate and metastasize (28), and the lack of periostin in damaged muscle may encourage mobilization and migration of satellite cells throughout the area of injury. Consistent with this working hypothesis, TGF-β is known to stimulate periostin secretion (11, 29), and inhibition of TGF-β leads to decreased periostin expression (7). In both skeletal and cardiac muscle, manipulation of TGF-β via a neutralizing antibody or treatment with losartan leads to improvement in muscle function and histology and, coincidently, a decrease in periostin in the muscle (7, 30). These results are consistent with the hypothesis that TGF-β secretion and its enhanced activity contribute to the demise of skeletal muscle in MD (9). However, one interesting possibility is that periostin functions as a key downstream effector of TGF-β that promotes its deleterious effects in MD (31). Indeed, in the absence of periostin, TGF-β appears to have a protective effect in MD disease progression by enhancing regeneration or by blunting other negative effects of this cytokine (14). The use of the TGF-β–blocking antibody worsened MD and resulted in greater functional decline in double-null mice. These findings support a complex interaction between periostin and TGF-β that may be related to the TGF-β paradox, where it can be both beneficial and deleterious depending on dosage and costimulatory factors (17).

Periostin expression in epithelial cells has been shown to stimulate TGF-β signaling and lead to enhanced collagen production and expression of matrix metalloproteinase 2 and MMP9 for further matrix remodeling (31). Thus, periostin may indirectly alter TGF-β–dependent disease signaling by changing the composition of the ECM with respect to other known TGF-β–binding proteins that reside there, such as the latent TGF-β–binding proteins, fibrillins, and thrombospondin-1, as well as by effecting interactions with select integrins that alter the function of latency-associated peptides in controlling how TGF-β is activated and presented to receptors on surrounding cells (32). Perturbation of TGF-β activity has been strongly implicated in the pathogenesis of diverse disease states, including MD. The incorporation of TGF-β antagonism into therapeutic strategies remains controversial, given the known mix of beneficial and deleterious effects. Our data presented here reveal the complexity of TGF-β signaling and suggest that selective targeting of downstream mediators of TGF-β, such as antiperiostin therapeutics, may be more optimal than global TGF-β inhibition.

Methods

Postn null mice were generated and characterized previously (19), as was the MD mouse model with deletion of the δ-sarcoglycan gene (21). Two mg/kg of TGF-β–blocking antibody (R&D Systems) was used in the blocking experiments and was given once a wk for a period of 6 wk. Histological analysis was performed using standard techniques, as elaborated in *SI Methods*.

ACKNOWLEDGMENTS. This work was supported by grants from the National Institutes of Health (to J.D.M. and E.M.M.) and the Howard Hughes Medical Institute (to J.D.M.). A.L. was supported by a Physician Scientist Award Pediatric Center Grant from the Institute of Child Health and Human Development.

1. Muir LA, Chamberlain JS (2009) Emerging strategies for cell and gene therapy of the muscular dystrophies. *Expert Rev Mol Med* 11:e18.
2. Kaplan JC (2009) Gene table of monogenic neuromuscular disorders (nuclear genome only). *Neuromuscul Disord* 19:77–98.
3. Bernasconi P, et al. (1999) Transforming growth factor-β1 and fibrosis in congenital muscular dystrophies. *Neuromuscul Disord* 9:28–33.
4. Chen YW, et al. (2005) Early onset of inflammation and later involvement of TGFβ in Duchenne muscular dystrophy. *Neurology* 65:826–834.
5. Gosselin LE, Martinez DA (2004) Impact of TNF-α blockade on TGF-β1 and type I collagen mRNA expression in dystrophic muscle. *Muscle Nerve* 30:244–246.
6. Gosselin LE, et al. (2004) Localization and early time course of TGF-β1 mRNA expression in dystrophic muscle. *Muscle Nerve* 30:645–653.
7. Cohn RD, et al. (2007) Angiotensin II type 1 receptor blockade attenuates TGF-β–induced failure of muscle regeneration in multiple myopathic states. *Nat Med* 13: 204–210.
8. Bedair HS, Karthikeyan T, Quintero A, Li Y, Huard J (2008) Angiotensin II receptor blockade administered after injury improves muscle regeneration and decreases fibrosis in normal skeletal muscle. *Am J Sports Med* 36:1548–1554.
9. Heydemann A, et al. (2009) Latent TGF-β–binding protein 4 modifies muscular dystrophy in mice. *J Clin Invest* 119:3703–3712.
10. Olson EN, Sternberg E, Hu JS, Spizz G, Wilcox C (1986) Regulation of myogenic differentiation by type β transforming growth factor. *J Cell Biol* 103:1799–1805.
11. Horiuchi K, et al. (1999) Identification and characterization of a novel protein, periostin, with restricted expression to periosteum and periodontal ligament and increased expression by transforming growth factor β. *J Bone Miner Res* 14:1239–1249.
12. Zinn K, McAllister L, Goodman CS (1988) Sequence analysis and neuronal expression of fasciclin I in grasshopper and *Drosophila*. *Cell* 53:577–587.
13. Marotta M, et al. (2009) Muscle genome-wide expression profiling during disease evolution in *mdx* mice. *Physiol Genomics* 37:119–132.
14. Kruzynska-Frejtag A, Machnicki M, Rogers R, Markwald RR, Conway SJ (2001) Periostin (an osteoblast-specific factor) is expressed within the embryonic mouse heart during valve formation. *Mech Dev* 103:183–188.
15. Shimazaki M, et al. (2008) Periostin is essential for cardiac healing after acute myocardial infarction. *J Exp Med* 205:295–303.
16. Oka T, et al. (2007) Genetic manipulation of periostin expression reveals a role in cardiac hypertrophy and ventricular remodeling. *Circ Res* 101:313–321.
17. Tian M, Schiemann WP (2009) The TGF-β paradox in human cancer: An update. *Future Oncol* 5:259–271.
18. Hack AA, et al. (2000) Differential requirement for individual sarcoglycans and dystrophin in the assembly and function of the dystrophin-glycoprotein complex. *J Cell Sci* 113:2535–2544.
19. Norris RA, Moreno-Rodriguez R, Hoffman S, Markwald RR (2009) The many facets of the matricelluar protein periostin during cardiac development, remodeling, and pathophysiology. *J Cell Commun Signal* 3:275–286.
20. Kii I, et al. (2010) Incorporation of tenascin-C into the extracellular matrix by periostin underlies an extracellular meshwork architecture. *J Biol Chem* 285:2028–2039.
21. Norris RA, et al. (2007) Periostin regulates collagen fibrillogenesis and the biomechanical properties of connective tissues. *J Cell Biochem* 101:695–711.
22. Bakay M, et al. (2006) Nuclear envelope dystrophies show a transcriptional fingerprint suggesting disruption of Rb-MyoD pathways in muscle regeneration. *Brain* 129: 996–1013.
23. Bakay M, Zhao P, Chen J, Hoffman EP (2002) A Web-accessible complete transcriptome of normal human and DMD muscle. *Neuromuscul Disord* 12(Suppl 1): S125–S141.
24. Pescatori M, et al. (2007) Gene expression profiling in the early phases of DMD: A constant molecular signature characterizes DMD muscle from early postnatal life throughout disease progression. *FASEB J* 21:1210–1226.
25. Kühn B, et al. (2007) Periostin induces proliferation of differentiated cardiomyocytes and promotes cardiac repair. *Nat Med* 13:962–969.
26. Lorts A, Schwanekamp JA, Elrod JW, Sargent MA, Molkentin JD (2009) Genetic manipulation of periostin expression in the heart does not affect myocyte content, cell cycle activity, or cardiac repair. *Circ Res* 104:e1–e7.
27. Katsuragi N, et al. (2004) Periostin as a novel factor responsible for ventricular dilation. *Circulation* 110:1806–1813.
28. Baril P, et al. (2007) Periostin promotes invasiveness and resistance of pancreatic cancer cells to hypoxia-induced cell death: Role of the β4 integrin and the PI3k pathway. *Oncogene* 26:2082–2094.
29. Snider P, et al. (2008) Periostin is required for maturation and extracellular matrix stabilization of noncardiomyocyte lineages of the heart. *Circ Res* 102:752–760.
30. Iekushi K, et al. (2007) Novel mechanisms of valsartan on the treatment of acute myocardial infarction through inhibition of the antiadhesion molecule periostin. *Hypertension* 49:1409–1414.
31. Sidhu SS, et al. (2010) Roles of epithelial cell-derived periostin in TGF-β activation, collagen production, and collagen gel elasticity in asthma. *Proc Natl Acad Sci USA* 107: 14170–14175.
32. Hynes RO (2009) The extracellular matrix: Not just pretty fibrils. *Science* 326: 1216–1219.